Lipid Nanoparticle Assisted mRNA Delivery for Potent Cancer Immunotherapy

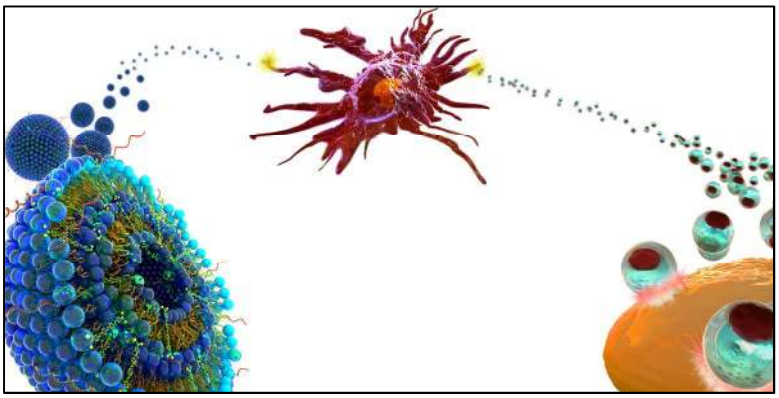

The induction of a strong cytotoxic T cell response is an important prerequisite for successful immunotherapy against many viral diseases and tumors. Nucleotide vaccines, including mRNA vaccines with their intracellular antigen synthesis, have been shown to be potent activators of a cytotoxic immune response. The intracellular delivery of mRNA vaccines to the cytosol of antigen presenting immune cells is still not sufficiently well understood. Here, we report on the development of a lipid nanoparticle formulation for the delivery of mRNA vaccines to induce a cytotoxic CD 8 T cell response. We show transfection of dendritic cells, macrophages, and neutrophils. The efficacy of the vaccine was tested in an aggressive B16F10 melanoma model. We found a strong CD 8 T cell activation after a single immunization. Treatment of B16F10 melanoma tumors with lipid nanoparticles containing mRNA coding for the tumor-associated antigens gp100 and TRP2 resulted in tumor shrinkage, and extended the overall survival of the treated mice. The immune response can be further increased by the incorporation of the adjuvant LPS. In conclusion, the lipid nanoparticle formulation presented here is a promising vector for mRNA vaccine delivery, one that is capable of inducing a strong cytotoxic T cell response. Further optimization, including the incorporation of different adjuvants, will likely enhance the potency of the vaccine.

KEYWORDS: mRNA, Lipid Nanoparticles, Vaccines, Immune Response, Cancer Immunotherapy, Cytotoxic T cells.

Cancer immunotherapy is based on the ability of the immune system to recognize and kill cancer cells.[1] Recent clinical trials testing checkpoint blockers or adoptive T cell transfer have shown that antigen specific T cells can control cancer.[2,3] To harness the immune system to treat cancer, one needs to develop strategies to neutralize tumor-promoting inflammation, to modify the tumor microenvironment that regulates T cell activity, and to broaden the T cell repertoire by vaccination.[4] The adaptive immune system acts to protect us from recurring infections through its two arms, the humoral arm, consisting of antibodies, and the cellular arm, consisting of T cells. Antibodies are a great tool to clear extracellular pathogens and toxins. However, for certain intracellular pathogens and tumors, specialized T cells, known as cytotoxic T Cells (CTLs) or cluster of differentiation 8 (CD 8) T cells, are needed.[5] Nucleotide vaccines with their ability to induce a strong Major Histocompatibility Complex I (MHC-I) mediated CD 8 T cell response are very attractive.[6] However, their delivery to target cells with minimal toxicity remains difficult.[7] Challenges for mRNA vaccine delivery include, mRNA has to: (a) be protected from degradation by omnipresent endonucleases, (b) reach the target cells, and (c) be both endocytosed and induce endosomal escape before degradation.[8,9] Various strategies have been advanced for successful mRNA vaccine delivery, such as encapsulation of mRNA in viral and nanoparticle vectors, or simply sequence optimization for increased stability and tailored immunogenicity.[9-12]

Our laboratory recently developed a library of lipid nanoparticles (LNPs) for the delivery of mRNA to hepatocytes.[13,14] Vectors for the intracellular delivery of oligonucleotides have been developed in various shapes and sizes. However, nanoparticles in a size range of up to about

200nm may be particularly well suited for the delivery of mRNA vaccines. Professional antigen presenting cells (APCs), especially dendritic cells (DCs), are important targets to induce T cell immunity.[15] APCs are enriched in the lymph nodes and continuously sample the draining interstitial fluid. For nanoparticles to be drained efficiently to the lymph nodes and be able to transfect APCs, the nanoparticle diameter, charge, and colloidal stability are all particularly important.[16,17] Compared to other vectors, LNPs offer a number of advantages, including: (i) LNP synthesis is robust, where both components and composition can be readily varied to increase delivery efficiency and reduce toxicity, (ii) immune potentiators, such as, adjuvants, or immune cell targeting ligands, can be incorporated to tailor the immune response, and (iii) LNPs have been successfully used in the past to deliver mRNA vaccines.[18-21] Remarkably, the earliest LNP formulation for the delivery of mRNA vaccines dates back to Martinon *et al.* in 1993.[22] Clinical experience with mRNA vaccines, so far, is very positive: No severe side effects have been reported, and an antigen specific immune response could be detected in some patients.[23-26] We are only aware of one clinical study involving lipid nanoparticles as an mRNA vector that reported results, and of one ongoing study.[20,27]

Our formulation consists of an ionizable lipid, a phospholipid, cholesterol, a polyethylene glycol (PEG) containing lipid, and an additive for the delivery of mRNA vaccines. The ionizable lipid is positively charged at low pH to allow complexation with the negatively-charged mRNA, and may also help with cellular uptake and endosomal escape.[28] The phospholipid and cholesterol are both important for the stability of the LNPs, and may also help with endosomal escape.[29,30] The PEGylated lipid hinders LNP aggregation, aids *in vivo* biodistribution, and reduces non-specific interactions.[31]

We hypothesized that LNPs from this library can be optimized for mRNA vaccine delivery for induction of a potent CD 8 T cell immune response.

To test the potential of expanding antigen specific T cell populations, there is no adequate *in vitro* assay. This follows because both T cell counts and antibody titers are 'second-order' effects that do not just depend on transfection efficiency of a particular type of immune cell, but also on the complex immunological signaling cascade which is necessary for an immune response to take place. Accordingly, a library of LNP formulations was optimized to induce a potent T cell response *in vivo*.

Table 1. Formulation Parameters for LNP Optimization. Lipid abbreviations: DOPE: 1,2-distearoyl-*sn*-glycero-3-phosphoethanolamine; DSPC: 1,2-distearoyl-*sn*-glycero-3-phosphocholine; POPE: 1-palmitoyl-2-oleoyl-*sn*-glycero-3-phosphoethanolamine; DMPC: 1,2-dimyristoyl-sn-glycero-3-phosphocholine; DOPS: 1,2-dioleoyl-*sn*-glycero-3-phospho-L-serine; DC-cholesterol: 3β-[N-(N',N'-dimethylaminoethane)-carbamoyl]cholesterol hydrochloride; C14-PEG2000: 1,2-dimyristoyl-*sn*-glycero-3-phosphoethanolamine-N-[methoxy(polyethylene glycol)-2000] (ammonium salt); C14-PEG350: 1,2-dimyristoyl-*sn*-glycero-3-phosphoethanolamine-N-[methoxy(polyethylene glycol)-350] (ammonium salt); C14-PEG1000: 1,2-dimyristoyl-*sn*-glycero-3-phosphoethanolamine-N-[methoxy(polyethylene glycol)-1000] (ammonium salt); C14-PEG3000: 1,2-dimyristoyl-*sn*-glycero-3-phosphoethanolamine-N-[methoxy(polyethylene glycol)-3000] (ammonium salt); C14-PEG2000: 1,2-distearoyl-*sn*-glycero-3-phosphoethanolamine-N-[methoxy(polyethylene glycol)-2000].

Component	Original Formulation	Library A	Library B
Ionizable Lipid	C12-200	C12-200, cKK-E12, 503O13, DOTAP, DODAP	cKK-E12
Molar Composition	31.5%	31.5%	10% to 35%
Phospholipid	DOPE	DOPE, DSPC, DOTAP, POPE, DMPC, DOPS	DOPE, DOPS
Molar Composition	10%	10%	7.5% to 47.5%
Cholesterol	Cholesterol	Cholesterol, DC-Cholesterol	Cholesterol
Molar Composition	36%	36%	35% to 61.5%
PEG-Lipid	C14-PEG1000	C14-PEG350, C14-PEG1000, C14-PEG2000, C14-PEG3000	C14-PEG2000
Molar Composition	2.5%	2.5%	2.5%
Additive	Arachidonic Acid	Arachidonic Acid, Oleic Acid, Myristic Acid, Sodium Lauryl Sulfate	Sodium Lauryl Sulfate
Molar Composition	20%	20%	0 to 16%

We developed an optimized LNP library complexed with mRNA coding for the model immunology protein ovalbumin (OVA) in groups of five C57BL/6 mice by subcutaneous injection in the lower back (dorsal posterior) at a dose of 10 μg of mRNA per mouse (**Figure 1A-C**). In the first phase of the optimization (Library A), we tested different lipids for the individual components: ionizable lipid, phospholipid, cholesterol, PEGylated lipid, and additive at a constant molar ratio (**Table 1**). The mice were bled seven days after a single injection, the red blood cells were lysed, and the monocytes were stained using a tetramer conjugate for the OVA-epitope SIINFEKL to determine the percentage of OVA specific CD8 T cells (**Figure 1D**). A list of the tested formulations and the corresponding CD 8 T cells levels are provided in the (**Table S1**). Among the ionizable lipids tested: C12-200, cKK-E12, 503O13, DOTAP, and DODAP, only cKK-E12 performed better than in the original formulation.[32] The two phospholipids (DSPC and DOPS), out of the six tested, performed better than DOPE did in the original formulation. However, using either phospholipid, 5 to 10 days after the immunization, more than 20% of the mice tested developed inflammation at the injection site. For this reason, we stopped using DSPC and DOPS. Formulations without phospholipid did not perform well at all: (Figure 1D, Formulation A-1). We also replaced cholesterol with DC-cholesterol, because it has been successfully used to formulate lipid nanoparticles for DNA plasmid and siRNA delivery.[33] However, we did not observe a higher percentage of OVA-specific CD 8 T cells using DC-cholesterol. By testing different PEG chain lengths, we found that the PEG length as well as the anchor lipid greatly influence the LNP diameter: C14-PEG350 (232nm), C14-PEG1000 (121nm), C14-PEG2000 (67nm), C18-PEG2000 (110nm), C14-PEG3000 (96nm), with the smallest LNP, C14-PEG2000, yielding the highest T cell levels. Arachidonic acid has been used to deliver LNPs carrying mRNA coding for Cas9.[34] However, in the case of vaccines, removal of

the arachidonic acid additive almost tripled the CD 8 T cell count. Interestingly, the SLS additive performed better than the no additive case. Based on the Library A screening, we identified cKK-E12 from formulation A-2, C14-PEG2000 from formulation A-12, and SLS from formulation A-18 as promising components for further investigation in Library B.

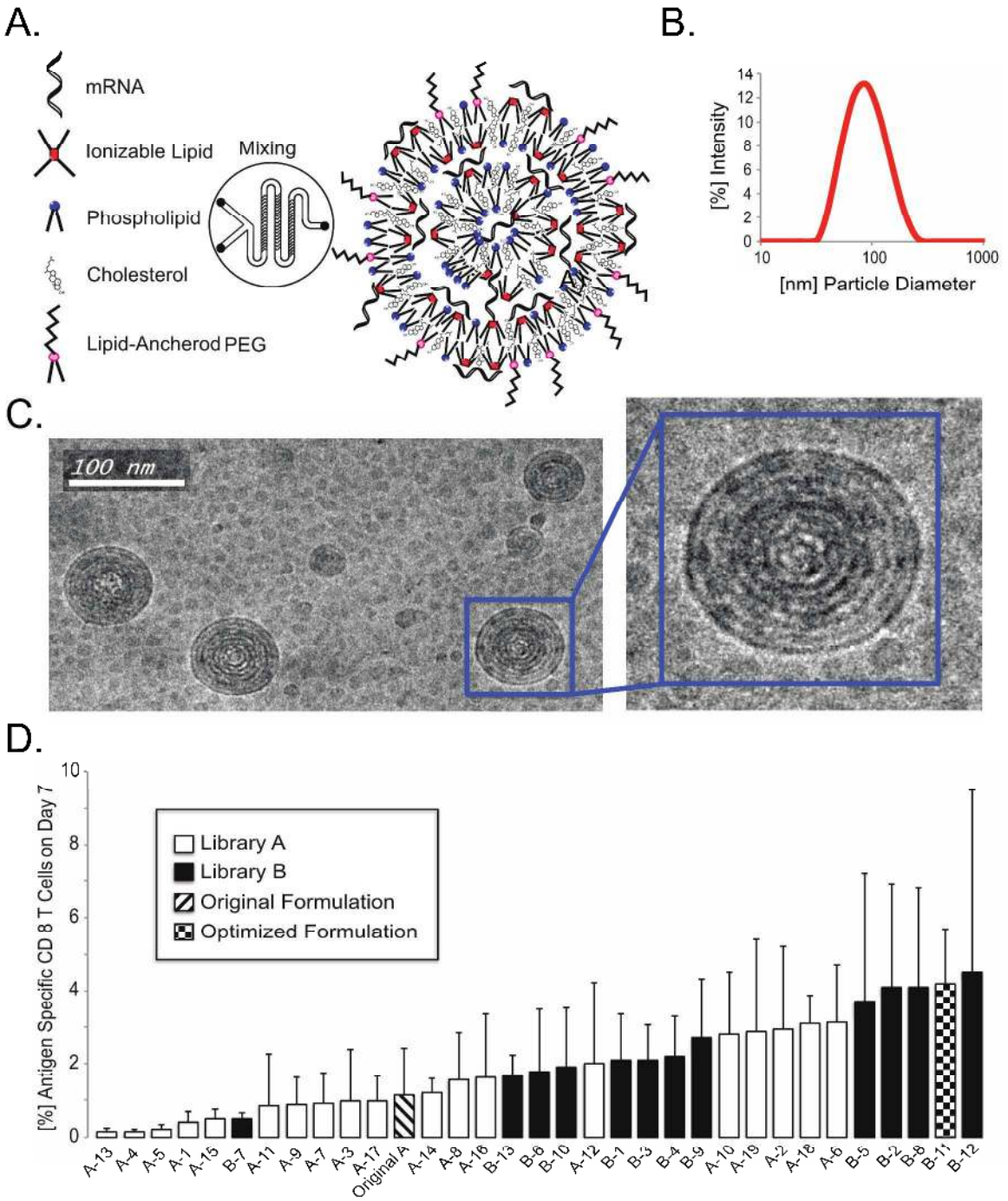

Figure 1: (A). A formulation of lipid nanoparticles is synthesized by mixing the aqueous phase containing the mRNA, and the ethanol phase containing the lipophilic compounds, using a microfluidic device. The ionizable lipid complexes with the negatively-charged mRNA at low pH, and can both facilitate endocytosis and endosomal escape. Phospholipid provides structural integrity to the bilayers, and can assist with endosomal escape of the mRNA to the cytosol. Cholesterol helps stabilize the LNPs and promotes membrane fusion. The lipid-anchored polyethylene glycol prevents LNP aggregation, and reduces non-specific interactions. (B) Size analysis of formulation B-11. Diameter distribution of the LNPs comprising the vaccine solution formulated with OVA mRNA, as determined using dynamic light scattering (DLS). (C) Cryogenic transmission electron microscopy image of the LNP solution suggests that the LNPs have spherical shape, and consist of a multi-lamellar structure. (D) In the first phase of the optimization (Library A; empty columns), different components were investigated, each at a constant molar composition. Percentage of OVA specific CD 8 T cells 7 days after the injection of 10 μg total mRNA per mouse are plotted for each formulation, including the original formulation (hatched column). The data is presented as mean + SD, n = 5. The three components, C14-PEG2000 (A-12), cKK-E12 (A-2), and SLS (A-18) in Library A were identified for further investigation in Library B (black columns). Combination of C14-PEG2000, cKK-E12, and SLS in different concentrations were tested to afford the optimized formulation B-11 patterned column).

In the second phase of the optimization (Library B), we combined the different individual components that we identified in the first phase as being beneficial (Library A), and investigated the effect of altering the molar compositions of the components. We found that varying the molar

composition of cKK-E12 correlated with detected CD8 T cell levels. Lower molar compositions of cKK-E12 led to increased T cell levels until 10 mol%, beyond which the deviation around the mean concentration of antigen specific CD 8 T cell levels increased significantly. (**Figure S1**) The particle sizes in the tested formulations ranged between 50nm and 150nm. In this particle size range, we could not establish a correlation between particle size and CD 8 T cell expansion (**Figure S3A**). The measured formulations had a negative zeta potential, and the highest CD 8 T cell expansions were observed with formulations having zeta potentials between -15 mV to -3 mV (**Figure S3B**). For either the molar compositions of DOPE and Cholesterol, we found no clear correlations between their molar compositions and the number of CD 8 T cells present. We then decided to further investigate the properties of formulation B-11 yielding the highest CD 8 T cell levels. To evaluate the locations of mRNA transfection and protein synthesis, we formulated firefly luciferase (FFL) mRNA in B-11 LNPs, and injected 10 μg of mRNA per mouse, as used in the vaccine study. 24 hours later, we used bioluminescence to detect the location of protein expression (**Figure 2A**). We found FFL expressed at the injection site and in the draining lymph nodes, in the inguinal lymph nodes, as well as in some axillary lymph nodes. Luminescence was not detected in the liver, spleen, lung, or intestines. We then monitored the protein expression of the 3 formulations A-1, A-6, and B-11 at the injection site over time (**Figure 2B and C**). It is noteworthy that all three formulations reached the expression maximum of about four orders of magnitude after 24 hours, and declined slowly afterwards. Formulation B-11 that elicited the highest CD 8 T cell levels did not translate into a higher maximal FFL concentration, compared to the other two formulations, but exhibited less drop-off in FFL concentration. All three formulations produced FFL for at least 10 days. The injection of the

same amount of unformulated mRNA led to an increase of one order of magnitude and dropped off rapidly.

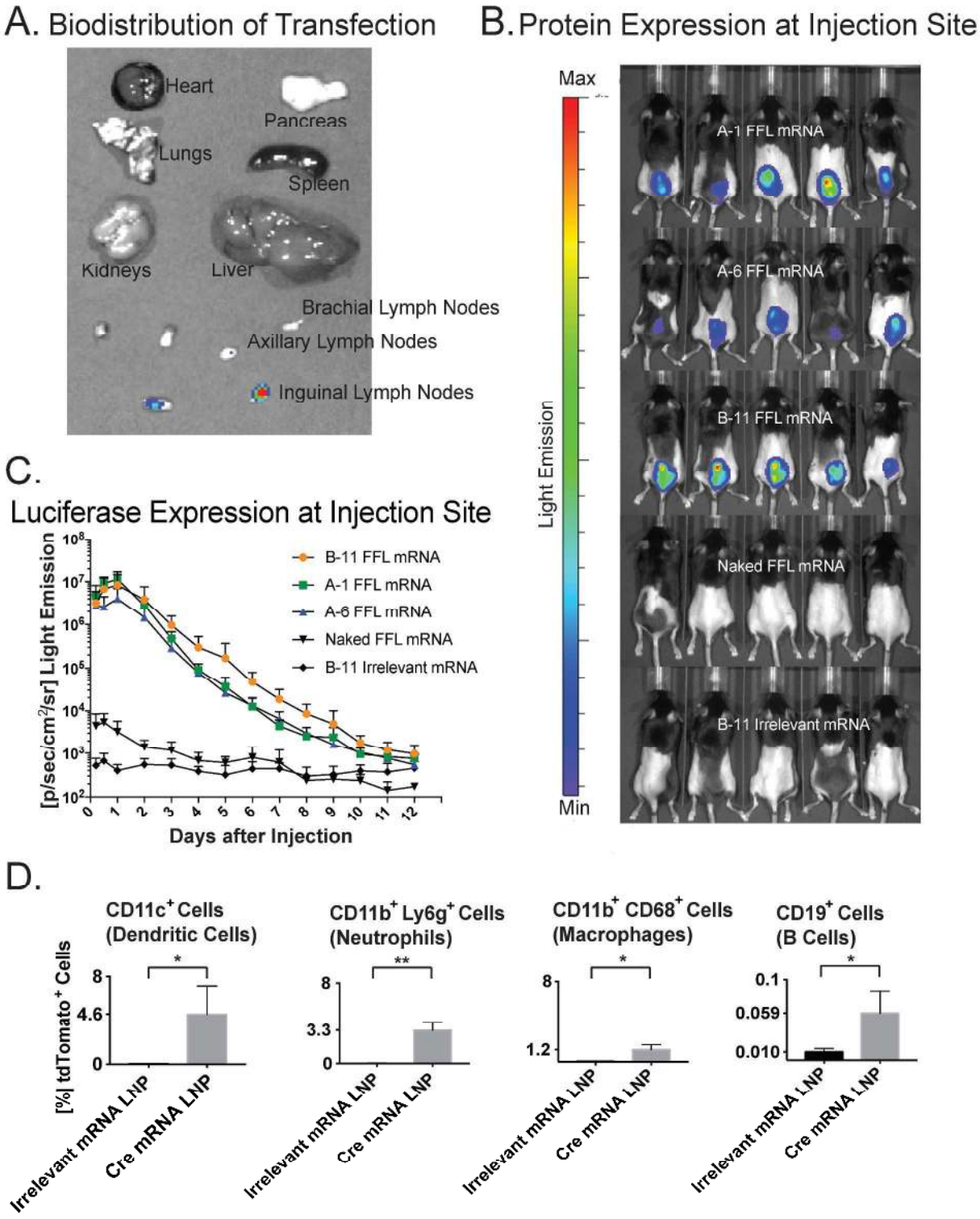

Figure 2. (A) Representative image of the biodistribution of luciferase expression using the B-11 formulation 24 h after subcutaneous injection. The inguinal and axillary lymph nodes emit light 24 h after injection. Importantly, no FFL expression is detected in the liver, kidney, spleen, colon, or lung. A sample set of mouse organs are analyzed 15 minutes after the injection of D-lucifein. (B) FFL encoding mRNA, formulated in different LNP formulations, unformulated (FFL) mRNA, and formulated irrelevant mRNA, were injected subcutaneously in the lower backs of mice. The FFL expression was visualized 24 h after injection by optical imaging. (C) Quantitative expression of FFL during 12 days. Formulation of mRNA in LNPs increases the FFL expression up to three orders of magnitude compared to unformulated mRNA. The FFL expression remains elevated for 10 days. Interestingly, the formulation yielding the highest CD8 T cell levels at day 7 does not exhibit a higher peak FFL expression, but exhibits a slower decrease over time. The corresponding antigen specific CD8 T cell levels at day 7 post injection using mRNA coding for ovalbumin (OVA, 10 μg per mouse, n=5 per group) are 1.1 ± 1.3% for Formulation A-1, 3.1 ± 1.6% for Formulation A-6, and 4.2 ± 1.5% for Formulation B-11. (D) Quantification of the percentage of transfected cells of the indicated type two days after the injection of LNPs containing mRNA coding for Cre-recombinase in Ai14D reporter mice, as determined by FACS analysis (n = 3 for control, and n = 4 for Cre LNP). *P<0.05, **P<0.01; unpaired student t test. The irrelevant control mRNA used in Figure 2 corresponds to mRNA coding for OVA.

To determine whether we are transfecting APCs, we used the Ai14D reporter mouse and LNPs containing mRNA coding for Cre-recombinase (**Figure 2D**). These mice harbor a mutation in the *Gt(ROSA)26Sor* locus with a *loxP*-flanked STOP cassette preventing transcription of a CAG

promoter driven tdTomato red fluorescent protein. Cells express tdTomato upon Cre-mediated recombination.[35] We have chosen the Ai14D reporter mouse because expression levels using commercially available mRNA coding for fluorescent proteins, such as GFP, toTomato, or cyan fluorescent protein, were below the detection levels for analysis using flow cytometry. The draining lymph nodes, the inguinal lymph nodes in this case were removed, digested, and the monocytes were stained with secondary antibodies. Flow cytometry revealed that 4.6% of DCs, 1.2% of macrophages, 3.3% of neutrophiles, and 0.06% of B cells expressed the Cre-recombinase.

Unmodified RNA has the potential to activate endosomal Toll-like receptors 3 (TLR3), TLR7, and TLR8.[36] Activation of these receptors induces an inflammatory response, transcription of pro-inflammatory cytokines, as well as up-regulation of chemokines and type I interferons. This effect is desirable for vaccine application, and activation of the immune system is necessary to initiate an immune response. However, other cytoplasmatic RNA sensors, such as cytoplasmic retinoic acid-inducible gene I (RIG-I) or protein kinase RNA-activated (PKR), may hinder translation and enhance RNA degradation.[8,37] In contrast to the immune activation, this effect of unmodified mRNA would be counter-productive for a strong immune response. Karikó *et al.* showed that by incorporating naturally occurring modified nucleosides, such as 5-methylcytidine, 5-methyluridine, 2-thiouridine, or pseudouridine, activation of the pattern recognition receptors can be suppressed.[38] We then compared the capacity of modified and unmodified mRNA formulations to elicit CD8 and CD4 T cell proliferations *in vivo*. We measured the CD8 and CD4 T cell levels in blood, six to eleven days after immunization, of mRNA coding for OVA unmodified and mRNA with the same nucleotide sequence, fully substituted with pseudouridine and 5-methylcytidine (**Figure 3A and 3B**).

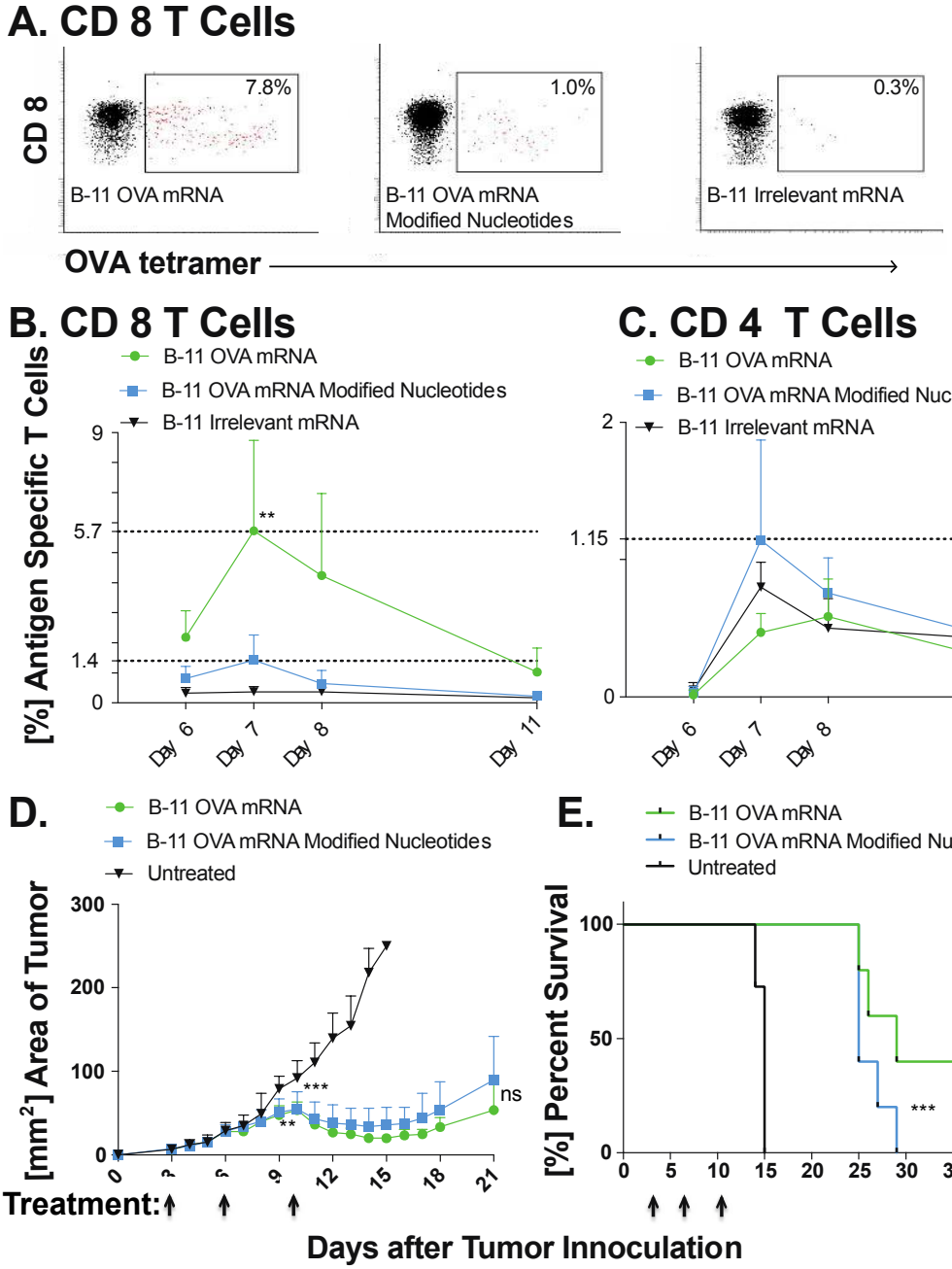
A. CD 8 T Cells
CD 8
7.8%
B-11 OVA mRNA
1.0%
B-11 OVA mRNA Modified Nucleotides
0.3%
B-11 Irrelevant mRNA
OVA tetramer
B. CD 8 T Cells
[%] Antigen Specific T Cells
B-11 OVA mRNA
B-11 OVA mRNA Modified Nucleotides
B-11 Irrelevant mRNA
9
5.7
1.4
0
**
Day 6
Day 7
Day 8
Day 11
C. CD 4 T Cells
2
1.15
0
D.
[mm2] Area of Tumor
Untreated
300
200
100
0
***
**
ns
Treatment:
E.
[%] Percent Survival
100
50
0
***
0 5 10 15 20 25 30 35 40
Days after Tumor Innoculation
F.
OVA Specific T Cells on Day 17
[%] OVA Specific CD 8 T Cells
ns
10
5
0
OVA Modified Nucleotides
OVA

Figure 3: C57Bl/6 mice (n=7) were immunized with mRNA LNPs (10 μg mRNA per mouse in 100 μL of PBS; the mRNA is either unmodified or completely substituted with 5-Methylcytidine (5meC) and Pseudouridine (ψ)), and subsequently, mice were bled at specific time points. The red blood cells were lysed and the monocytes were stained with tetramer, live-dead stain, CD4 and CD8 antibody conjugates. (A) Representative FACS profiles of mice treated with the indicated conditions. The CD8 T cell response in peripheral blood is much stronger from unmodified mRNA LNP vaccines. (B) The percentage of OVA specific CD8 T cells peaks at day 7 after subcutaneous injection. Compared to unmodified mRNA, the substitution with 5meC and ψ induces an immune response only slightly higher that in the group treated with irrelevant control mRNA LNPs. mRNA coding for β-galactosidase was used as the irrelevant control. (** $P < 0.01$ by ordinary one-way ANOVA Bonferroni's multiple comparisons test) (C) No significant increase in circulating antigen specific CD 4 T cells could be detected. (D) mRNA LNP formulation B-11 induces potent *in vivo* antitumor immunity. Mice (C57BL/6J, n = 10 for the control group and n = 5 for the treated mice) were injected subcutaneously in the upper back with 1 x 10^5 B16-OVA melanoma cells on day 0. Treatment began when tumors were clearly visible in all mice (day 3) with LNP formulation B-11 containing OVA mRNA either modified or unmodified (days 3, 6, and 10, 10 μg total mRNA per mouse and injection). Both treatment groups slow down tumor growth after the second treatment, and shrink the tumor after the third treatment. Mice that reached the maximal allowed tumor area of 250 mm^2, or that developed ulceration, were euthanized and recorded as having tumor areas of 250mm^2 (** $P < 0.01$, *** $P < 0.001$, as compared with the untreated control group, two-way ANOVA with Bonferroni post-hoc). (E) Overall survival is increased for both treatment groups. Statistical analysis was done using a log rank analysis (*** $P<0.001$, as compared with the untreated control group, Mantel

Cox test. The two mRNA treated groups are not significantly different). (F) The percentage of SIINFEKL specific CD 8 T cells that were analyzed on day 17, the difference in CD 8 T cells was not statistically significant.

For both modified and unmodified mRNA, when compared with irrelevant mRNA, similarly formulated, we did not find much difference in the CD 4 T cell levels at any time point. On the other hand, the CD8 T cells present a very different picture. Specifically, while the CD 8 T cell levels for modified mRNA differ from the control only on day 7, mice treated with unmodified mRNA LNPs exhibited much higher CD 8 T cell levels at all time points measured. Modified mRNA containing LNP-treated mice reached 1.4% on day 7 not statistically significant from the control, while mice treated with unmodified mRNA LNPs reached a 5.7% ($P = 0.003$) significantly higher level of CD 8 T cells on day 7. This increase may be attributed to the activation of the innate immune system pattern recognition receptors, inducing inflammation, such as type I interferon. In this regard, our data are in agreement with two recently published articles investigating the role of type I interferon after intravenous injection of LNP mRNA vaccines.[20,21] Both studies suggest that type I interferon is necessary for a protective CD8 T cell response. We also measured the antigen specific IgG titers 7 weeks after a single immunization (**Figure S2**). Only at a serum dilution of 1:16 or smaller, OVA specific IgG serum antibody titers were more than a standard deviation different from those in the control mice that were immunized with LNPs containing an irrelevant control mRNA.

To address the functionality of the proliferated CD 8 T cells, we tested formulation B-11 in a transgenic OVA-expressing tumor immunotherapy model to evaluate whether proliferated CD 8 T cells induce potent antitumor function. To this end, we injected mice with 10^5 of B16-OVA

melanoma cells, and began treatment on day 3 after tumor inoculation, when tumors were visible and palpable in all mice. The treatment consisted of a total of 3 injections of either modified or unmodified OVA mRNA LNPs (10 μg of mRNA per mouse per injection) in formulation B-11. We decided to choose a dosing schedule similar to what has been published by the mRNA company CureVac. For therapeutic cancer immunotherapy applications they dosed successfully in 3 to 4 day intervals.[39] We treated the mice on days 3, 6, and 10 and compared them against an untreated control group (**Figure 3D**). Mice treated with either modified or unmodified mRNA LNPs had slower tumor growth and even tumor shrinkage for up to 7 days after the last treatment. We measured the CD 8 T cell levels seven days after the last treatment, and found them to be higher for the group treated with LNPs containing unmodified mRNA (**Figure 3F**). To test our formulations with antigens other than OVA, we investigated the B16F10 melanoma model and encapsulating mRNA encoding for two well described and widely studied melanoma self-antigens: tyrosinase-related protein 2 (TRP2)[40] and a point-mutated version of glycoprotein 100 (gp100)[41]. In this version of gp100, the serine in position 27 is exchanged to a proline. We chose self-antigens because it has been shown that overcoming self-tolerance can be very difficult, and we hypothesized that our formulation would be potent enough to overcome that.[42]

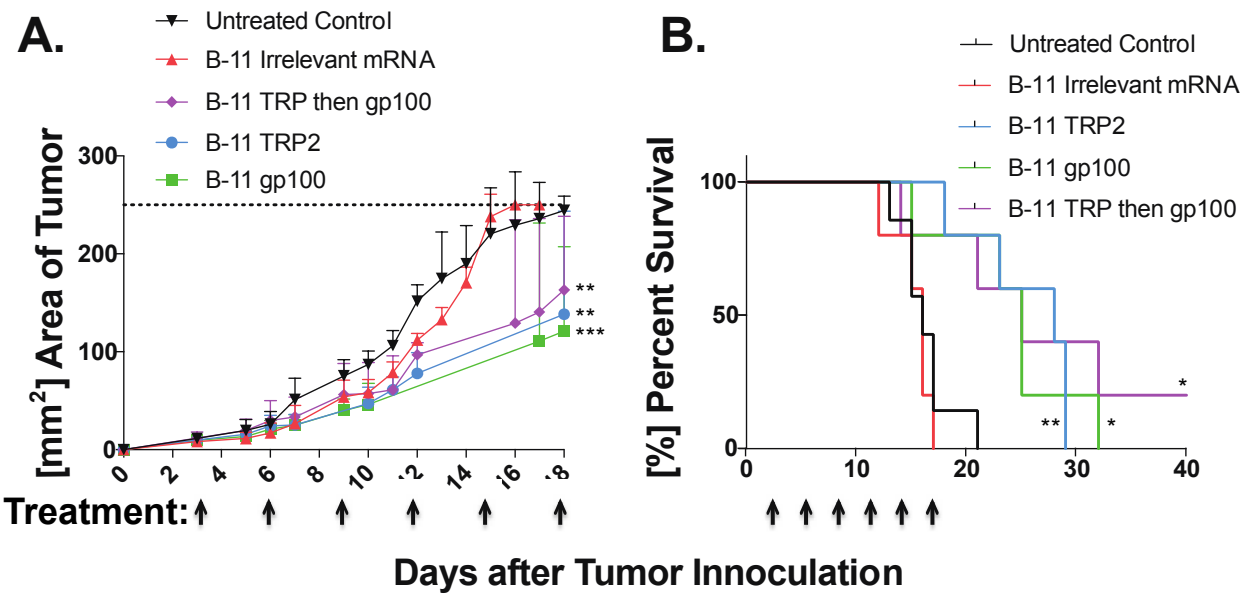

Figure 4. mRNA LNPs coding for tumor self-antigens, gp100 and TRP2, slow down tumor growth and extend overall survival. Mice (C57BL/6J, n=7 for untreated control and n=5 per other groups) were inoculated with 10^5 of B16F10 melanoma cells, and treated began when tumors were visible in all mice on day 3. Treatment consisted of a subcutaneous injection of LNP formulation B-11 encapsulation the indicated mRNA (10 μg of total mRNA per mouse in 0.1 mL of sterile PBS). All the treated mice receive 6 injections with 3-day intervals starting on day 3 after the tumor inoculation. The groups included 6 treatments with gp100, TRP2, irrelevant control mRNA, 3 treatments with TRP2 followed by 3 treatments with gp100, and an untreated control group. (A) Tumor areas were measured with a caliper lengths x width. Mice that reached the maximal allowed tumor area of 250 mm^2, or that developed ulceration, were euthanized and recorded as having tumor areas of 250mm^2. All 3 treatment groups showed slower tumor growths (** $P < 0.01$, *** $P < 0.001$, as compared with either control group, two-way ANOVA with Bonferroni post-hoc). (B) All 3 treated groups survived significantly longer the either the untreated control group or mice treated with irrelevant mRNA. One mouse in the group treated 3 times with TRP2 mRNA containing LNPs, followed by 3 treatments of gp100 mRNA containing

LNPs, survived 60 days (the end of the study) without visible tumors. (* $P < 0.05$, ** $P < 0.01$, as compared with the untreated control group, Mantel Cox test). LNPs containing mRNA coding for OVA were used as irrelevant controls to generate Figure 4.

The B16F10 tumor model has been used previously in the context of mRNA LNP vaccines. Perche et al. showed that two immunizations with mRNA LNPs could extend overall survival in a prophylactic immunotherapy setting[43] and Kranz et al. used a B16F10-Luc lung metastasis model and showed complete rejection of lung metastasis upon vaccination with TRP-1 mRNA lipoplex.[20] The untreated and irrelevant control mRNA mice all died within three weeks. (**Figure 4B**) All 3 treatment groups resulted in longer overall survivals: mice treated with either gp100, TRP2, and mice treated 3 times with TRP2, followed by 3 times with gp100. One mouse in the latter group survived for 60 days until the end of the study without any visible tumors.

We then tested the hypothesis if enhanced TLR activation could increase the potency of the immune response by incorporating an adjuvant in the LNP formulation. We replaced 1% of the molar composition of PEG in the optimized LNP formulation with lipopolysaccharide (LPS, 10 μg per mL), consisting of a lipid A anchor, an inner core, an outer core, and an *O*-antigen repeat.[44] LPS is a very potent TLR4 agonist.[45] We envisioned that the LPS anchors in the outer membrane of the LNPs via the lipid A anchor, and points the highly hydrophobic *O*-antigen repeat outward. An additional benefit of replacing some of the shielding PEG with *O*-antigen repeat carbohydrates may be that the LNPs bind to APCs via carbohydrate recognizing lectin receptors that are omnipresent on APCs and are endocytosed more efficiently.[18] Dendritic cells express a number of lectins on their surfaces that allow ligand capture and endocytosis. These include the mannose receptor[46], Langerin also known as CD207[47], Dec-205[48], DC-SIGN also

known as CD209[49], Dectin-1, and Dectin-2.[50] The CD 4 T cell kinetics was not different from those observed in either treatment group. (**Figure S4**) The observed CD 8 T cell levels peaked one day after the non-LPS LNPs on day 8 at 6.3% antigen specific CD 8 T cells. (**Figure 5A**) It is noteworthy that LPS-containing LNPs may induce local inflammation at LPS concentrations of more than 1.0 μg per mouse. We then added LPS to LNPs containing TRP2 mRNA, and tested them in the B16F10 melanoma model. We found that the mice receiving the LPS containing TRP2 mRNA LNPs survived significantly longer compared to the controls and mice receiving TRP2 mRNA LNPs. (**Figure 5B and 5C**)

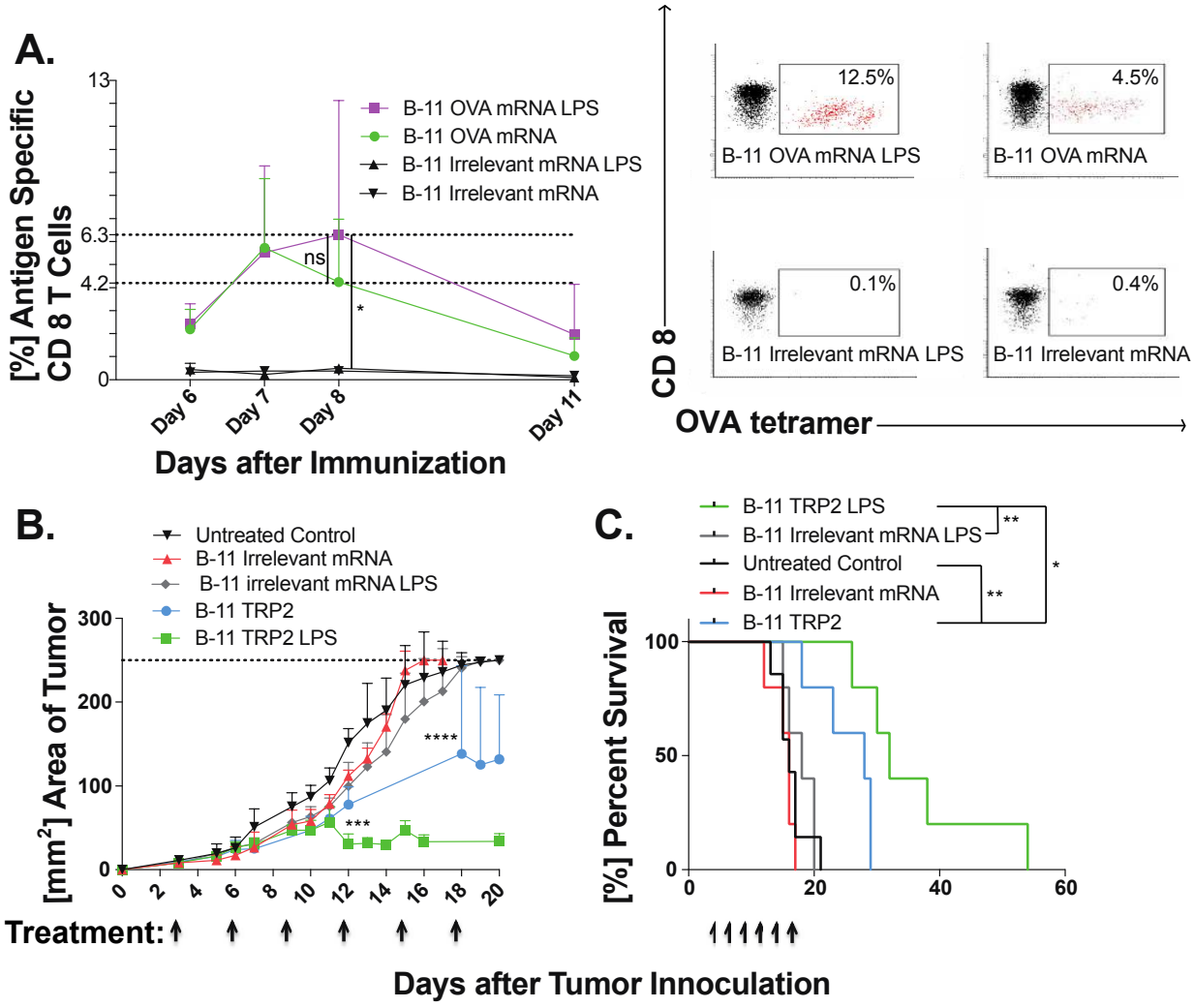

Figure 5. Incorporating LPS in the LNPs increases both the CD 8 T cell levels and anti-tumor activity. LNPs were formulated at the same lipid ratio as formulation B-11, but 1 mol-percent of PEG was replaced with 1 mol-percent of LPS. (A) Left: LNPs containing 1.0 μg of LPS per dose, formulated with OVA mRNA, increase the CD8 T cell levels 8 days after the immunization. Right: Representative FACS profiles day 8. (* $P < 0.05$ by ordinary one-way ANOVA Bonferroni's multiple comparisons test). (B) In the B16 F10 tumor model, LPS containing LNPs, formulated with TRP2 mRNA, induce tumor shrinkage as compared to the slower tumor growth by TRP2 mRNA formulated in the B-11 formulation. (*** $P < 0.001$, **** $P < 0.0001$, as compared with the B-11 irrelevant mRNA LPS group, two-way ANOVA with Bonferroni post-hoc). (C) The LPS containing LNPs lead to longer overall survival. (* $P < 0.05$, ** $P < 0.01$, as compared with the untreated control group, Mantel Cox test). β-Galactosidase mRNA was used as the irrelevant control for the studies reported in Figure 5).

In conclusion, we presented evidence that our optimized LNP formulation, B-11, works well for delivering mRNA vaccines. Using the Ai14D reporter mice and the B-11 LNP formulation, we showed transfection in different immune cell populations, including dendritic cells, macrophages, neutrophils, and B cells. Cytosolic antigen synthesis and degradation by the proteasome enables antigen presentation on MHC-I, and consequently, activation of a potent CD 8 T cell response. We did not only induce CD 8 T cell proliferation, but the killer cells were also functional, as shown by extending the overall survival in a transgenic mouse melanoma model. Even more exciting was the effect on the aggressive B16F10 tumor model, where mRNA coding for the tumor associated self-antigens, TRP2 and gp100, was able to overcome the self-tolerance and to significantly extend the overall mice survival. The fact that adding LPS to the LNP

formulation further increased survival is an indication that such additions may increase the potency of mRNA vaccines delivered by LNPs. The proof of concept presented here warrants further investigation of LNPs as potentially useful mRNA vaccine vectors

Materials and Methods. *Lipid Nanoparticle (LNP) Synthesis.* LNPs were synthesized by mixing an aqueous phase containing the mRNA with an ethanol phase containing the lipids in a microfluidic chip device as described previously.[51] Briefly, the aqueous phase was prepared in 10 mM citrate buffer (pH 3) with corresponding mRNA (OVA, FFL, Cre, gp100, and TRP2, 1mg/mL in 10mM TRIS-HCl, from Trilink Biotechnologies, San Diego, CA). The ethanol phase was prepared by solubilizing a mixture of ionizable lipid, phospholipid, cholesterol, lipid-anchored PEG, and additive at predetermined molar ratios. For the LPS containing formulations, the LPS was added to the ethanol phase as a solution in DMSO (1 mg/mL; Lipopolysaccharide from *E. coli* 055:B5, purified by ion-exchange chromatography; Sigma-Aldrich order number L4524). Syringe pumps were used to mix the ethanol and aqueous phases at a 3:1 ratio in a microfluidic chip device. The resulting LNPs were dialyzed against PBS in a 20 000 MWCO cassette at room temperature for 2 h. The lipids used were obtained from: 1,2-dioleoyl-3-trimethylammonium-propane (DOTAP, Avanti Polar Lipids, Alabaster, AL), 1,2-dioleoyl-3-dimethylammonium-propane (DODAP, Avanti), C12-200 (prepared as previously described[28]), cKK-E12 (prepared as previously described[32]), 503O13 (prepared as previously described[52]), 1,2-distearoyl-*sn*-glycero-3-phosphoethanolamine (DOPE, Avanti), 1,2-distearoyl-*sn*-glycero-3-phosphocholine (DSPC, Avanti), 1-palmitoyl-2-oleoyl-*sn*-glycero-3-phosphoethanolamine (POPE, Avanti), 1,2-dimyristoyl-sn-glycero-3-phosphocholine (DMPC, Avanti), 1,2-dioleoyl-*sn*-glycero-3-phospho-L-serine (DOPS, Avanti), cholesterol (Sigma-Aldrich, St. Louis, MO), 3β-

[N-(N',N'-dimethylaminoethane)-carbamoyl]cholesterol hydrochloride (DC-cholesterol, Avanti), 1,2-dimyristoyl-*sn*-glycero-3-phosphoethanolamine-N-[methoxy(polyethylene glycol)-2000] (ammonium salt) (C14-PEG2000, Avanti), 1,2-dimyristoyl-*sn*-glycero-3-phosphoethanolamine-N-[methoxy(polyethylene glycol)-350] (ammonium salt) (C14-PEG350, Avanti), 1,2-dimyristoyl-*sn*-glycero-3-phosphoethanolamine-N-[methoxy(polyethylene glycol)-1000] (ammonium salt) (C14-PEG1000, Avanti), 1,2-dimyristoyl-*sn*-glycero-3-phosphoethanolamine-N-[methoxy(polyethylene glycol)-3000] (ammonium salt) (C14-PEG3000, Avanti), 1,2-distearoyl-*sn*-glycero-3-phosphoethanolamine-N-[methoxy(polyethylene glycol)-2000] (ammonium salt) (C18-PEG2000, Avanti), sodium lauryl sulfate (SLS, sigma-Aldrich), arachidonic acid (Sigma-Aldrich), oleic acid (Sigma-Aldrich), myristic acid (Sigma-Aldrich).

LNP Characterization. The size and polydispersity index (PDI) of the LNPs were measured using dynamic light scattering in 1X PBS (ZetaPALS, Brookhaven Instruments) (**Table 2**). Zeta potentials were measured using the same instrument in a 0.1X PBS solution. Diameters are reported as the largest intensity mean peak average, which constitutes >95% of the nanoparticles present in the sample. To calculate the nucleic acid encapsulation efficiency, a modified Quant-iT RiboGreen RNA assay (Invitrogen) was used as previously described.[53]

Table 2. Characterization of LNP formulations used in the manuscript.

Formulation	mRNA	Diameter [nm]	PDI	Zeta Potential [mV]	Z-Average [nm]
B-11	FFL	108	0.232	-8.9	96.0

B-11	OVA	88	0.171	-10.2	76.4
B-11	OVA modified	84	0.123	-4.7	73.2
B-11 with LPS	OVA	97	0.165	-14.1	82.5
B-11	β-Gal	93	0.177	-2.9	82.0
B-11 with LPS	β-Gal	102	0.174	2.0	91.7

Cryo-Transmission Electron Microscopy. To prepare LNPs for Cryo-Transmission Electron Microscopy (TEM), they were dialyzed against 0.1X PBS in a 20 000 MWCO cassette for 2 h. 3 μL of the LNP solution was dropped on a lacey copper grid coated with a continuous carbon film and blotted to remove excess sample without damaging the carbon layer by Gatan Cryo Plunge III. A grid was mounted on a Gatan 626 single tilt cryo-holder equipped in the TEM column. The specimen and holder tip were cooled down by liquid nitrogen during transfer into the microscope and subsequent imaging. Imaging on a JEOL 2100 FEG microscope was done using minimum dose method. This is essential to avoid sample damage under the electron beam. The microscope was operated at 200 kV, and with a magnification in the range of 10 000~60 000 to assess particle diameter and distribution. All images were recorded on a Gatan 2kx2k UltraScan CCD camera.

Mice. All procedures were performed under an animal protocol approved by the Massachusetts Institute of Technology Committee on Animal Care (CAC), and in accordance with the guidelines for animal care in a MIT animal facility. C57BL/6J mice and B6.Cg-

Gt(ROSA)$^{26Sortm14(CAG-tdTomato)Hze}$/J (Ai14D) mice, 6 to 8 weeks of age, were purchased from Jackson Laboratories and housed in an MIT animal facility.

Immunization. Mice were anesthetized in a ventilated anesthesia chamber with 2.5% isofluorane in oxygen. The lower back of the mice were shaved with a clipper and the LNPs (0.1 mL containing 10 μg of mRNA per mouse) were injected subcutaneously in the lower back of the mice. Mice were put back in their cages, and monitored for signs of distress and local inflammation at the injection site.

Bioluminescence. 24 h after the injection of the mRNA LNPs, mice were injected subcutaneously at the injection site with 0.1 mL of D-luciferin (10 mg/mL in PBS). The mice were anesthetized in a ventilated anesthesia chamber with 2.5% isofluorane in oxygen, and imaged 20 minutes after the injection with an in-vivo imaging system (IVIS, Perkin Elmer, Waltham, MA). Luminescence was quantified using the LivingImage software (Perkin Elmer).

Flow Cytometric Analysis. At different time points after the immunization, blood was collected via mouse tail vein, and the red blood cells were lysed using a RBC lysis buffer solution (eBioscience, San Diego, CA). The Monocytes were incubated with Fc block (CD16/32, BioLegend, diluted in FACS buffer at 1:9) at 4°C for 15 minutes. The monocytes were then incubated for 30 minutes at room temperatures with PE conjugates of MHC tetramers specific for either CD4 T cells recognizing the OVA epitope ISQAVHAAHAEINEAGR (MBL International, Woburn, MA), CD 8 T cells recognizing the OVA epitope SIINFEKL (MBL International), CD 8 T cells recognizing the gp 100 epitope EGSRNQDWL (MBL International), or CD 8 T cells recognizing the TRP2 epitope SVYDFFVWL (MBL International). Subsequently, the cells were incubated for 10 minutes at room temperature with a Propidium

iodide staining solution (eBioscience, diluted in FACS buffer 1:25), CD4-e450 (eBioscience, diluted in FACS buffer 1:200), and CD8α-APC (eBioscience, diluted in FACS buffer 1:200). The cells were washed with FACS buffer and data was collected on a BD LSR II.

Ai14D Reporter Mice Transfection Analysis. Ai14D mice were immunized with B-11 LNPs containing mRNA coding for either Cre-recombinase or irrelevant mRNA. The draining lymph nodes, the inguinal lymph nodes were removed and digested in a medium containing Collagenase D (1mg/mL, Roche Diagnostics, Indianapolis, IN) for 90 minutes at 37 °C. The solution was then filtered through a 70 μm mesh and centrifuged. The cells were resuspended at 4 °C in staining buffer for 30 minutes at 4 °C. The staining buffer contained antibodies specific for the cell markers: CD68–PerCP/Cy5.5; CD19–Alexa Fluor 647; CD11b–BV 421; Ly-6G–FITC; CD11c–APC; and CD16/32. The samples were analyzed after three washes on a BD LSR II HTS-2 flow cytometer.

Enzyme-Linked Immunosorbent Assay (ELISA) for Antigen-Specific OVA Serum Antibody Detection. Lockwell Maxisorp plates (Thermo Scientific, Waltham, MA) were coated overnight at 4 °C with 44 μL/well of OVA (InvivoGen, San Diego, CA), 5 mg/mL in 100 mMol carbonate/bicarbonate buffer, pH 9.6), and blocked for 1 h at 37 °C with 200 μL of blocking solution (5% BLOTTO, (Santa Cruz Biotechnology, Dallas, TX), in PBS containing 0.05% Tween20, (Sigma-Aldrich). Serum samples were initially diluted 1:16 in a carrier solution (same as blocking solution), transferred into coated-blocked plates, and serially 2-fold diluted. The plates were incubated for 2 h at 37 °C, washed and incubated with a detection antibody: goat anti mouse IgG HRP conjugate (Santa Cruz Biotechnology, diluted 1:1000 in carrier solution) and

washed again. Antigen-specific total IgG was detected with HRP substrate ODP (Sigma-Aldrich) and read at 490/630nm using an infinite M1000 plate reader (Tecan, Switzerland).

Tumor Cell Lines. B16-OVA is a murine B16F10 cell line that stably expresses chicken egg ovalbumin (OVA). The cell line was a kind gift from Dr. Kenneth Rock, Dana-Farber Cancer Institute, Boston. B16F10 melanoma cell line was obtained from ATCC. Both cell lines were maintained in DMEM, supplemented with fetal bovine serum (10%).

ASSOCIATED CONTENT

Supporting Information Available: [Additional experimental data and analysis.] This material is available free of charge via the Internet at http://pubs.acs.org.

AUTHOR INFORMATION

Corresponding Author

*Massachusetts Institute of Technology, Room 66-442b, 77 Massachusetts Avenue, Cambridge, MA, 02139-4307, USA, Phone: +1 617 253 4594, Fax: +1 617 252 1651, E-mail: dblank@mit.edu

Present Addresses

†If an author's address is different than the one given in the affiliation line, this information may be included here.

Notes

Robert Langer is co-founder and member of the board of directors of Moderna Therapeutics. The authors have no other relevant affiliations or financial involvement with any organization or entity with a financial interest in, or financial conflict with, the subject matter or materials discussed in the manuscript apart from those disclosed.

ACKNOWLEDGMENT

We would like to acknowledge the core facilities in the David H. Koch Institute for Integrative Cancer Research at the Massachusetts Institute of Technology. In particular, we would like to thank Glen A. Paradis from the flow cytometry core facility, and Yun Dong Soo from the nano core facility. This work was supported by an Innovation Grant from the Ragon Institute of MGH, MIT, and Harvard. MAO and MJM were supported by a fellowship of the Max Planck Society. The authors would like to thank Trilink Biotechnologies for a gift of mRNA coding for OVA, OVA modified with 5meC and Ψ, TRP2, and gp100. We also acknowledge a gift of LPS from Sigma-Aldrich. MJM is supported by a Burroughs Wellcome Fund Career Award at the Scientific Interface, a Ruth L. Kirschstein National Research Service Award (F32CA200351) from the National Institutes of Health (NIH), and a grant from the Burroughs Wellcome Fund (no. 1015145).

REFERENCES

(1) Dunn, G. P.; Old, L. J.; Schreiber, R. D. *Annu. Rev. Immunol.* **2004**, *22*, 329–360.

(2) Sharma, P.; Allison, J. P. *Science* **2015**, *348*, 56–61.

(3) Rosenberg, S. A.; Restifo, N. P. *Science* **2015**, *348*, 62–68.

(4) Palucka, A. K.; Coussens, L. M. *Cell* **2016**, *164*, 1233–1247.

(5) Butterfield, L. H. *BMJ* 2015;350:h988.

(6) Melief, C. J. M.; van Hall, T.; Arens, R.; Ossendorp, F.; van der Burg, S. H. *J. Clin. Invest.* **2015**, *125*, 3401–3412.

(7) Kauffman, K. J.; Webber, M. J.; Anderson, D. G. *J. Controlled Release* **2015**, *240*, 227–234.

(8) Sahin, U.; Karikó, K.; Türeci, O. *Nat. Rev. Drug. Discov.* **2014**, *13*, 759–780.

(9) Yin, H.; Kanasty, R. L.; Eltoukhy, A. A.; Vegas, A. J.; Dorkin, J. R.; Anderson, D. G. *Nat. Rev. Genet.* **2014**, 15, 541–555.

(10) Yamamoto, A.; Kormann, M.; Rosenecker, J.; Rudolph, C. Eur. *J. Pharm. Biopharm.* **2009**, *71*, 484–489.

(11) Hoerr, I.; Obst, R.; Rammensee, H. G.; Jung, G. *Eur. J. Immunol.* **2000**, *30*, 1–7.

(12) Carralot, J.-P.; Probst, J.; Hoerr, I.; Scheel, B.; Teufel, R.; Jung, G.; Rammensee, H. G.; Pascolo, S. *Cell. Mol. Life Sci.* **2004**, *61*, 2418–2424.

(13) Kauffman, K. J.; Dorkin, J. R.; Yang, J. H.; Heartlein, M. W.; DeRosa, F.; Mir, F. F.; Fenton, O. S.; Anderson, D. G. *Nano Lett.* **2015**, *15*, 7300–7306.

(14) Fenton, O. S.; Kauffman, K. J.; McClellan, R. L.; Appel, E. A.; Dorkin, J. R.; Tibbitt, M. W.; Heartlein, M. W.; DeRosa, F.; Langer, R.; Anderson, D. G. *Adv. Mater. (Weinheim, Ger.)* **2016**, *28*, 2939–2943.

(15) Trumpfheller, C.; Longhi, M. P.; Caskey, M.; Idoyaga, J.; Bozzacco, L.; Keler, T.; Schlesinger, S. J.; Steinman, R. M. *J. Intern. Med.* **2012**, *271*, 183–192.

(16) Manolova, V.; Flace, A.; Bauer, M.; Schwarz, K.; Saudan, P.; Bachmann, M. F. *Eur. J. Immunol.* **2008**, *38*, 1404–1413.

(17) Reddy, S. T.; Rehor, A.; Schmoekel, H. G.; Hubbell, J. A.; Swartz, M. A. *J. Controlled Release* **2006**, *112*, 26–34.

(18) Midoux, P.; Pichon, C. *Expert Rev. Vaccines* **2015**, *14*, 221–234.

(19) Reichmuth, A. M.; Oberli, M. A.; Jeklenec, A.; Langer, R.; Blankschtein, D. *Ther. Delivery* **2016**, *7*, 319–334.

(20) Kranz, L. M.; Diken, M.; Haas, H.; Kreiter, S.; Loquai, C.; Reuter, K. C.; Meng, M.; Fritz, D.; Vascotto, F.; Hefesha, H.; Grunwitz, C.; Vormehr, M.; Hüsemann, Y.; Selmi, A.; Kuhn, A. N.; Buck, J.; Derhovanessian, E.; Rae, R.; Attig, S.; Diekmann, J.; Jabulowsky, R. A.; Heesch, S.; Hassel, J.; Langguth, P.; Grabbe, S.; Huber, C.; Türeci, O.; Sahin, U. *Nature* **2016**, *534*, 396–401.

(21) Broos, K.; Van der Jeught, K.; Puttemans, J.; Goyvaerts, C.; Heirman, C.; Dewitte, H.; Verbeke, R.; Lentacker, I.; Thielemans, K.; Breckpot, K. *Mol. Ther. Nucleic Acids* **2016**, *5*, e326.

(22) Martinon, F.; Krishnan, S.; Lenzen, G.; Magné, R.; Gomard, E.; Guillet, J. G.; Lévy, J. P.; Meulien, P. *Eur. J. Immunol.* **1993**, *23*, 1719–1722.

(23) Weide, B.; Carralot, J.-P.; Reese, A.; Scheel, B.; Eigentler, T. K.; Hoerr, I.; Rammensee, H.-G.; Garbe, C.; Pascolo, S. *J. Immunother.* **2008**, *31*, 180–188.

(24) Weide, B.; Pascolo, S.; Scheel, B.; Derhovanessian, E.; Pflugfelder, A.; Eigentler, T. K.; Pawelec, G.; Hoerr, I.; Rammensee, H.-G.; Garbe, C. *J. Immunother.* **2009**, *32*, 498–507.

(25) Rittig, S. M.; Haentschel, M.; Weimer, K. J.; Heine, A.; Muller, M. R.; Brugger, W.; Horger, M. S.; Maksimovic, O.; Stenzl, A.; Hoerr, I.; Rammensee, H.-G.; Holderried, T. A. W.; Kanz, L.; Pascolo, S.; Brossart, P. *Mol. Ther.* **2011**, *19*, 990–999.

(26) Rittig, S. M.; Haentschel, M.; Weimer, K. J.; Heine, A.; Muller, M. R.; Brugger, W.;

Horger, M. S.; Maksimovic, O.; Stenzl, A.; Hoerr, I.; Rammensee, H.-G.; Holderried, T. A.; Kanz, L.; Pascolo, S.; Brossart, P. *Oncoimmunology* **2016**, *5*, e1108511.

(27) Clinical Trials Registry of the U. S. National Institute of Health. https://clinicaltrials.gov/ct2/show/NCT02410733?term=biontech&rank=1 (accessed Sept. 1, 2016).

(28) Love, K. T.; Mahon, K. P.; Levins, C. G.; Whitehead, K. A.; Querbes, W.; Dorkin, J. R.; Qin, J.; Cantley, W.; Qin, L. L.; Racie, T.; Frank-Kamenetsky, M.; Yip, K. N.; Alvarez, R.; Sah, D. W. Y.; de Fougerolles, A.; Fitzgerald, K.; Koteliansky, V.; Akinc, A.; Langer, R.; Anderson, D. G. *Proc. Natl. Acad. Sci.* U. S. A. **2010**, *107*, 1864–1869.

(29) Zuhorn, I.; Bakowsky, U.; Polushkin, E.; Visser, W.; Stuart, M.; Engberts, J.; Hoekstra, D. *Mol. Ther.* **2005**, *11*, 801–810.

(30) Allen, T. M.; Cullis, P. R. *Adv. Drug Delivery Rev.* **2013**, *65*, 36-48.

(31) Mui, B. L.; Tam, Y. K.; Jayaraman, M.; Ansell, S. M.; Du, X.; Tam, Y. Y. C.; Lin, P. J.; Chen, S.; Narayanannair, J. K.; Rajeev, K. G.; Manoharan, M.; Akinc, A.; Maier, M. A.; Cullis, P.; Madden, T. D.; Hope, M. J. *Mol. Ther. Nucleic Acids* **2013**, *2*, e139.

(32) Dong, Y.; Love, K. T.; Dorkin, J. R.; Sirirungruang, S.; Zhang, Y.; Chen, D.; Bogorad, R. L.; Yin, H.; Chen, Y.; Vegas, A. J.; Alabi, C. A.; Sahay, G.; Olejnik, K. T.; Wang, W.; Schroeder, A.; Lytton-Jean, A. K. R.; Siegwart, D. J.; Akinc, A.; Barnes, C.; Barros, S. A.; Carioto, M.; Fitzgerald, K.; Hettinger, J.; Kumar, V.; Novobrantseva, T. I.; Qin, J.; Querbes, W.; Koteliansky, V.; Langer, R.; Anderson, D. G. *Proc. Natl. Acad. Sci.* U. S. A. **2014**, *111*, 3955–3960.

(33) Wyrozumska, P.; Meissner, J.; Toporkiewicz, M.; Szarawarska, M.; Kuliczkowski, K.; Ugorski, M.; Walasek, M. A.; Sikorski, A. F. *Cancer Biol. Ther.* **2014**, *16*, 66–76.

(34) Yin, H.; Song, C.-Q.; Dorkin, J. R.; Zhu, L. J.; Li, Y.; Wu, Q.; Park, A.; Yang, J.; Suresh, S.; Bizhanova, A.; Gupta, A.; Bolukbasi, M. F.; Walsh, S.; Bogorad, R. L.; Gao, G.; Weng, Z.; Dong, Y.; Koteliansky, V.; Wolfe, S. A.; Langer, R.; Xue, W.; Anderson, D. G. *Nat. Biotechnol.* **2016**, *34*, 328–333.

(35) Madisen, L.; Zwingman, T. A.; Sunkin, S. M.; Oh, S. W.; Zariwala, H. A.; Gu, H.; Ng, L. L.; Palmiter, R. D.; Hawrylycz, M. J.; Jones, A. R.; Lein, E. S.; Zeng, H. *Nat. Neurosci.* **2009**, *13*, 133–140.

(36) Jensen, S.; Thomsen, A. R. *J. Virol.* **2012**, *86*, 2900–2910.

(37) Pollard, C.; Rejman, J.; De Haes, W.; Verrier, B.; Van Gulck, E.; Naessens, T.; De Smedt, S.; Bogaert, P.; Grooten, J.; Vanham, G.; De Koker, S. *Mol. Ther.* **2013**, *21*, 251–259.

(38) Karikó, K.; Buckstein, M.; Ni, H.; Weissman, D. *Immunity* **2005**, *23*, 165-175.

(39) Fotin-Mleczek, M.; Duchardt, K. M.; Lorenz, C.; Pfeiffer, R.; Ojkić-Zrna, S.; Probst, J.; Kallen, K.-J. *J. Immunother.* **2011**, *34*, 1–15.

(40) Parkhurst, M. R.; Fitzgerald, E. B.; Southwood, S.; Sette, A. *Cancer Res.* **1998**, *58*, 4895–4901.

(41) van Stipdonk, M. J. B.; Badia-Martinez, D.; Sluijter, M.; Offringa, R.; van Hall, T.; Achour, A. *Cancer Res.* **2009**, *69*, 7784–7792.

(42) Pedersen, S. R.; Sørensen, M. R.; Buus, S.; Christensen, J. P.; Thomsen, A. R. *The J. Immunol.* **2013**, *191*, 3955–3967.

(43) Perche, F.; Benvegnu, T.; Berchel, M.; Lebegue, L.; Pichon, C.; Jaffrès, P.-A.; Midoux, P. *Nanomedicine* **2011**, *7*, 445–453.

(44) Raetz, C.; Whitfield, C. *Annu. Rev. Biochem.* **2002**, *71*, 635-700.

(45) Brubaker, S. W.; Bonham, K. S.; Zanoni, I.; Kagan, J. C. *Annu. Rev. Immunol.* **2015**, *33*, 257–290.

(46) Martinez-Pomares, L. *J. Leukocyte Biol.* **2012**, *92*, 1177–1186.

(47) van der Vlist, M.; Geijtenbeek, T. B. H. *Immunol. Cell Biol.* **2010**, *88*, 410–415.

(48) Mahnke, K.; Guo, M.; Lee, S.; Sepulveda, H.; Swain, S. L.; Nussenzweig, M.; Steinman, R. M. *J. Cell Biol.* **2000**, *151*, 673–684.

(49) Geijtenbeek, T. B. H.; Engering, A.; Van Kooyk, Y. *Immunol. Cell Biol.* **2002**, *71*, 921–931.

(50) Dambuza, I. M.; Brown, G. D. *Curr. Opin. Immunol.* **2015**, *32*, 21–27.

(51) Chen, D.; Love, K. T.; Chen, Y.; Eltoukhy, A. A.; Kastrup, C.; Sahay, G.; Jeon, A.; Dong, Y.; Whitehead, K. A.; Anderson, D. G. *J. Am. Chem. Soc.* **2012**, *134*, 6948–6951.

(52) Whitehead, K. A.; Dorkin, J. R.; Vegas, A. J.; Chang, P. H.; Veiseh, O.; Matthews, J.; Fenton, O. S.; Zhang, Y.; Olejnik, K. T.; Yesilyurt, V.; Chen, D.; Barros, S.; Klebanov, B.; Novobrantseva, T.; Langer, R.; Anderson, D. G. *Nat. Commun.* **2014**, *5*, 4277.

(53) Heyes, J.; Palmer, L.; Bremner, K.; MacLachlan, I. *J. Controlled Release* **2005**, *107*, 276–287.